Eur. Phys. J. B **59**, 451–456 (2007)
DOI: 10.1140/epjb/e2007-00305-2

THE EUROPEAN PHYSICAL JOURNAL B

Quantum simulations of spin-relaxation and transport in copper

K.P. McKenna[1,2,a] and G.J. Morgan[3]

[1] Department of Physics and Astronomy, University College London, Gower Street, London, WC1E 6BT, UK
[2] London Centre for Nanotechnology, 17-19 Gordon Street, London, WC1H 0AH, UK
[3] School of Physics and Astronomy, E.C. Stoner Laboratory, University of Leeds, Leeds. LS2 9JT, UK

Received 8 September 2007
Published online 15 November 2007 –

Abstract. A quantum equation of motion method is applied to simulate conduction electron spin-relaxation and transport in the presence of the spin-orbit interaction and disorder. A spin-relaxation time of 25ps is calculated for Cu with a realistic low temperature resistivity of 3.2 $\mu\Omega$cm – corresponding to a spin-diffusion length of about 0.4 μm. Spin-relaxation in a finite nanocrystallite of Cu is also simulated and a short spin-relaxation time (0.47 ps) is calculated for a crystallite with 7% surface atoms. The spin-relaxation calculated for bulk Cu is in good agreement with experimental evidence, and the dramatic nanocrystallite effect observed has important implications for nano-spintronic devices.

PACS. 72.25.Ba Spin polarized transport in metals – 73.63.-b Electronic transport in nanoscale materials and structures – 72.25.Hg Electrical injection of spin polarized carriers

1 Introduction

Given the subject of this topical issue it is scarcely necessary to expound the interest and applications of spintronics (spin-electronics) and spin transfer. The ability to pass non-equilibrium spin-polarised currents through inhomogeneous nanoscale heterostructures offers numerous possibilities in terms of novel device functionality – giant magnetoresistive (GMR) hard disk read heads, magnetic random access memory and SpinFETs (spin field effect transistors) are just a few important examples [1–3]. Furthermore, the prospect spin-currents present to actively manipulate the macroscopic magnetisation orientation of nanomagnets within such devices opens up many more device possibilities [4]. One can envisage architectures which would combine the SpinFET paradigm with the ability to store information in a non-volatile way within a single device. The advantages this may provide over existing technologies are numerous and exciting – and this is in part responsible for the increasing interest in the subject.

The successful application of spintronic devices rely upon the control and maintained coherence of spin-currents. Effects which give rise to the decay of spin-currents by spin-flip scattering are therefore of central importance. Spin-flip scattering can be caused by impurities (magnetic or not), dislocations, grain-boundaries, magnons in ferromagnetic materials close to or above the Curie temperature and also the intrinsic spin-orbit interaction of conduction electrons. A detailed discussion of spin-flip mechanisms in a range of materials can be found in [5]. In this article we focus on spin-relaxation and transport in copper as this is an important material of broad interest. Copper is often used as a spacer layer separating ferromagnetic components in many spintronic systems, such as Co/Cu/Co GMR devices. For Cu and other similar paramagnetic metals the spin-flip mechanism is dominated by the intrinsic spin-orbit interaction of the conduction electrons [5] – a fact which is reflected by the much stronger spin-flip scattering observed in gold compared to copper. In this article we report simulations of the spin-relaxation of conduction electrons caused by the spin-orbit interaction using a quantum-mechanical equation-of-motion method [6]. We also demonstrate the simulation of spin-injection into Cu using the same formalism which is an important development as it allows dynamic effects to be treated.

2 Background

The spin-orbit interaction is a consequence of relativistic effects which become important close to the nucleus of an atom. Core electrons, which are fairly well localised, experience large spin-orbit interactions whereas valence electrons are affected relatively weakly. The Dirac equation includes relativistic effects and when expanded to first order contains three terms in addition to the standard kinetic energy and potential found in the Schrödinger equation [7]. Two of the terms (the mass-velocity and Darwin corrections) give rise to changes in the eigenenergies, which

[a] e-mail: k.mckenna@ucl.ac.uk

are usually quite small. The other term, the spin-orbit interaction, is often rewritten in the form, $\zeta(r)\,\mathbf{L}.\mathbf{S}$, by assuming the potential to be spherically symmetric and the function,

$$\zeta(r) = \frac{\hbar^2}{4m^2c^2}\frac{1}{r}\frac{\partial V}{\partial r}\,, \tag{1}$$

can be regarded as a spin-orbit potential and is large where the potential, V, varies rapidly close to the nucleus. As its name suggests it is an interaction which can give rise to non-zero matrix elements between the spin and orbital components of a wavefunction.

An important consequence of the spin-orbit interaction for periodic systems is that the eigenfunctions are not Bloch functions containing only one pure spin state. Instead, the Bloch states are spinors with components which contain mixtures of the two pure spin states – for example,

$$\Psi_\uparrow = [a_\mathbf{k}|\uparrow\rangle + b_\mathbf{k}|\downarrow\rangle]e^{i\mathbf{k}\cdot\mathbf{r}}\,, \tag{2}$$

where $a_\mathbf{k}$ and $b_\mathbf{k}$ are two different functions with the periodicity of the lattice [8]. If the spin-orbit strength is weak the eigenfunctions are formed predominantly of one pure spin ($|b_\mathbf{k}|^2 \ll |a_\mathbf{k}|^2$). The proportion of opposite spin that is mixed into the states depends upon the strength of the spin-orbit coupling and the proximity of bands which the state can couple to at the same wave-vector.

In a periodic system the spin-orbit interaction cannot cause spin-relaxation, however in the presence of disorder it can. Disorder or temperature, or any mechanism that destroys translational symmetry, gives rise to finite matrix elements between spin-eigenstates and hence spin-relaxation. The spin-relaxation rate can be related to the momentum scattering rate using quite simple assumptions about the electronic structure and first order perturbation theory. It can be shown that the spin-relaxation rate is directly proportional to the resistivity [8,9], ρ,

$$\frac{1}{\tau_{\mathrm{sf}}} \propto \frac{1}{\tau} \propto \rho\,, \tag{3}$$

where τ_{sf} is the spin-flip scattering time, and τ is the momentum scattering time. This mechanism for spin-relaxation is known as the Elliott-Yafet mechanism and is the most important mechanism for copper and similar metals.

Fabian and Das Sarma introduced the idea of spin hot-spots to explain the anomalously high spin-relaxation rate observed in some metals – Al for instance [10]. If there are regions of the Fermi surface where bands accidentally come close together, there is a large increase in the spin-relaxation rate. This is because perturbation theory predicts a relaxation rate that goes as,

$$\frac{1}{\tau_{\mathrm{sf}}} \propto \frac{1}{\Delta E}\,, \tag{4}$$

where ΔE is the separation between the Fermi energy and a band to which the spin can couple to at the same wave-vector. Similar effects occur at special symmetry points or where the Fermi surface crosses the Brillouin zone boundary. These so called spin-hot-spots can have relaxation rates that are orders of magnitude larger than on the rest of the Fermi surface. They occupy only a very small fraction of the total Fermi surface, but these small regions can dominate the overall spin-relaxation as typically the momentum scattering rate is several thousand times faster than the spin-relaxation rate in metals. Electrons will sample most of the Fermi surface before flipping their spin. The spin-orbit interaction itself modifies the band structure in such a way as to make spin-hot-spots less important for many metals, but such effects can be very important in polyvalent metals such as Al.

Spin-relaxation in metals has been probed experimentally using a number of different techniques. The transverse spin-lattice relaxation time (T_2) can be extracted from the line width in conduction electron spin resonance (CESR) experiments [11]. Spin-relaxation has also been measured by examining the magneto-optical response of a system following excitation by a fast magnetic field pulse [12] and in this case the longitudinal spin-lattice relaxation time is probed (T_1). A number of transport measurements have also enabled an estimation of the spin-relaxation time indirectly. This is based upon measuring a resistance which is dependent upon the spin-polarisation [13] and invoking ideas about spin-diffusion based upon solutions of the Boltzmann equation [14].

3 Methods

In order to simulate electronic transport and spin-relaxation quantum-mechanically an equation-of-motion (EOM) is used. The electronic structure is represented by a parameterised tight-binding model [15] which can account for complex electronic structures, such as transition metals for example, but allows large systems to be considered. The method is numerically stable in a variety of situations and has been described in some detail previously where GMR in a Co/Cu/Co multilayer was calculated [6], but here we review the main points.

The EC potential, Φ, is the relevant potential for electron transport in metals in the absence of magnetic fields. It consists of the electrostatic potential due to space charge, ϕ, together with the chemical potential, μ, due to variation of electron density. In equilibrium, currents due to density gradients must balance currents due to internal electric fields. It follows that in the case of a homogeneous system with constant and uniform electric field the conductivity, σ and the diffusion coefficient, D, must be related through the Einstein relation [16],

$$\sigma = e^2 g(E_{\mathrm{F}})\, D, \tag{5}$$

where $g(E_{\mathrm{F}})$ is the density of states at the Fermi energy. Chemical potential gradients are therefore equivalent to electrostatic potential gradients in linear response – despite the fact that the former does not accelerate electrons. Therefore it is very convenient to neglect the electrostatic potential and calculate the conductance by simulating electron diffusion. If a particle current, I, and

a chemical potential difference, $\Delta\mu$, is calculated between two points, then the conductance can be obtained using,

$$G = \frac{Ie^2}{\Delta\mu}. \tag{6}$$

A tight-binding (TB) basis set is used as the short range hopping integrals lead to nearly diagonal matrices and hence large systems may be studied easily. The wavefunction in the TB approximation takes the following form,

$$\Psi(\mathbf{r}) = \sum_{\gamma} a_\gamma \phi_\gamma(\mathbf{r}), \tag{7}$$

where a_γ is a complex amplitude associated with each orbital. In this abbreviated notation the suffix γ denotes an atomic orbital on a particular site with a given spin eigenstate, given by the orbital wavefunction $\phi_\gamma(\mathbf{r})$. The parameterized TB electronic structure model employed has hopping matrix elements that have been used as fitting parameters to agree with more accurate band structure calculations [15]. A two-center orthogonal representation containing s-, p-, and d-orbitals is used and yields electronic structures that are in reasonable agreement with more numerically demanding methods.

The time dependent Schrödinger equation (TDSE) can be integrated numerically to simulate the dynamics of electrons passing through the system. Appropriate boundary conditions must be used in order to set up the non-equilibrium current and these are discussed in detail elsewhere [6]. The TB TDSE that must be numerically integrated takes a particularly simple functional form,

$$i\hbar\frac{\partial}{\partial t}a_\gamma(t) - a_\gamma(t)E_\gamma - \sum_{\gamma'} a_{\gamma'}(t)V_{\gamma\gamma'} = 0, \tag{8}$$

where $V_{\gamma\gamma'}$ are hopping matrix elements between the various orbitals which in general can depend on time, and E_γ are orbital energies. The state of the system at any instant in time is completely specified by the set of complex amplitudes, $a_\gamma(t)$.

In order to account for spin-relaxation caused by the spin-orbit interaction of the conduction electrons a simple prescription is used. Working within the TB framework one should expect the wavefunction and potential close to the nucleus should be very similar to that in the free isolated atom – in contrast to a pseudopotential picture for example. It should hence be a reasonable approximation to take spin-orbit parameters as calculated for free-atoms [8]. The spin-orbit interaction in TB form couples opposite spins in p, d and higher orbitals according to symmetry constraints. However opposite spins in s orbitals are not coupled – it is essential to use a more complex TB model than one containing just s-states to account for spin-orbit effects correctly.

Atomic spin-orbit constants have been calculated using a self-consistent Hartee-Fock (SCHF) method by Herman and Skillman [17] and we use these parameters in our calculations. The spin-orbit constant, ξ_l, depends upon the

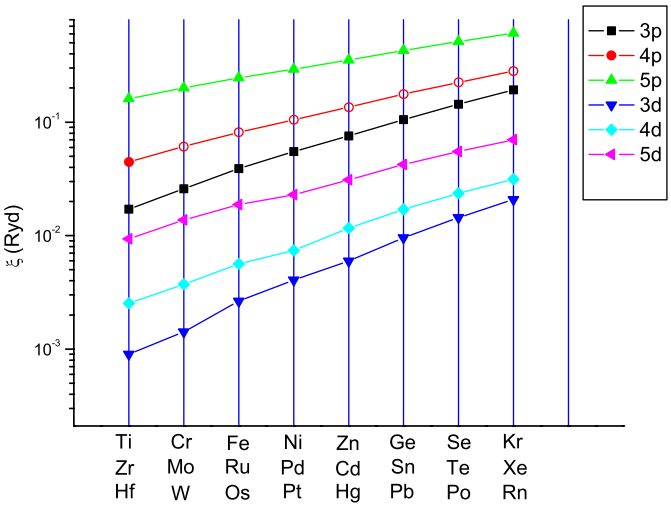

Fig. 1. Dependence of valance electron spin-orbit interaction accross the periodic table as calculated by SCHF [17].

the material and on the angular momentum, l, of the orbital and is defined in the following way,

$$\xi_l = \int_0^\infty \left[r^2 f_l(r)\right]^2 \zeta(r)\, r^2 dr, \tag{9}$$

where $f_l(r)$ is the radial part of the atomic wavefunction. Although $f_l(r)$ has a very different form in the free atom to in the crystal the short range of $\zeta(r)$ (Eq. (1)) ensures that the atomic approximation remains very reasonable. In the solid state orbitals which are unoccupied in the atom can also contribute to the valence band but obtaining corresponding spin-orbit parameters is not straighforward. The simple approach taken in this work is to use the spin-orbit parameters for the highest occupied p- and d-orbitals. This allows us to develop our methodology and to investigate trends but it should be noted that it may lead to an overestimation of the spin-orbit interaction strength. This may be improved upon by performing additional SCHF calculations. The atomic spin-orbit parameters for the highest occupied p- and d-orbitals are shown in Figure 1 for elements across the centre of the periodic table, which goes approximately as $Z^{\frac{3}{2}}$. The SCHF calculations were performed for closed shells, but other elements can be interpolated easily. The form of the matrix elements between tight-binding d-orbitals have been worked out by Friedel [18] in terms of the constants, ξ. The p-orbital matrix elements have been deduced in analogous way have been included into the tight-binding parameterisations.

In order to calculate the spin-relaxation rate we directly simulate the time evolution of a spin-polarised density using the EOM method. A region of material is considered and at time $t = 0$ a wavefunction is initialised on the lattice by assigning random phases on all sites, $a_\gamma = e^{i\phi_\gamma}$. Such a wavefunction has all eigenstates occupied with equal probability on the average. This wavefunction must be augmented so that only eigenstates close to the Fermi energy are present so that the spin-relaxation

simulated corresponds to conduction electrons under low bias conditions. This is achieved using a filtering technique used commonly in the evaluation of the Kubo formula [19]. The filtered wavefunction is obtained by time-integrating the initial wavefunction with an appropriate filter function, $F(E,t)$, in the following way,

$$\Psi^F = \int_0^\infty F(t)\,\Psi(t)\,dt\,. \tag{10}$$

The filter function can be selected to pick out a Lorentzian, Gaussian or indeed any distribution of states, however in this work a filter function that was proposed by Hickey [20] is used,

$$F(t) = \frac{1}{\pi}\frac{1}{\sqrt{2W}}\frac{\sin(Wt)}{t}e^{iE_0 t}\,, \tag{11}$$

which selects states within an energy window, W, of E_0 with a 'top-hat' distribution. In practice the filter integration is of course truncated at a finite time, T_F, and consequently the filter window is modified. In practice we find that $T_\mathrm{F} > 5000$ Ryd^{-1} produces a well defined window for a width, $W = 0.01$ Ryd.

After the filtering procedure the norm of the wavefunction per spin is proportional to the DOS at the Fermi energy. On the average there is no chemical potential difference between the two spin channels and the system is in equilibrium. In order to calculate a spin-relaxation time one of the spin channels can be excited – simply by multiplying the wavefunction amplitudes by a constant factor, for example multiplying $a_\gamma^\uparrow$ by a factor of 2. This creates a chemical potential difference between the spin channels due to the density difference. The state of the system can be evolved in time using the TDSE (Eq. (8)) and the spin-polarisation will relax to equilibrium providing spin-flip mechanisms are present. This type of simulated relaxation corresponds directly to magneto-optical measurements [12] and probes the longitudinal spin-relaxation time.

4 Results

4.1 Spin relaxation in Cu

A Cu cube with fcc structure and lattice constant 3.61 Å is considered which contains 13500 atoms and periodic boundary conditions are applied in all directions. The on-site energies are Anderson disordered [21] in order to account for electron scattering and all orbitals, s, p and d, are characteried by the same width of the on-site energy distribution, W. A realistic resistivity for copper at low helium temperatures is 3.2 $\mu\Omega$cm, corresponding to an Anderson disorder with a full width spread of $W = 0.5$ eV [22]. Spin-relaxation in copper is simulated using the methods that have been outlined above with, $\zeta_p = -0.0654$ Ryd and $\zeta_d = -0.0050$ Ryd, used for the TB spin-orbit constants. A filter window of 0.1 eV is used and a filter time of $T_\mathrm{F} = 5000$ Ryd^{-1}. Subsequent to the spin-imbalance the EOM is integrated numerically for 50,000 Ryd^{-1} (or 2.9 ps).

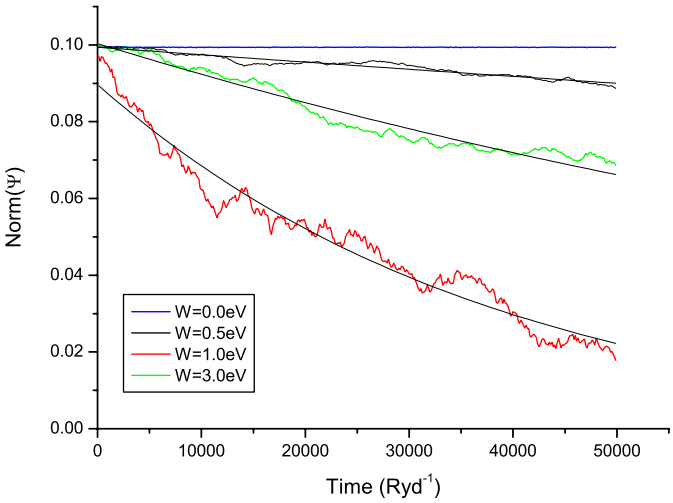

Fig. 2. Spin relaxation in Cu with periodic boundary conditions and different levels of disorder, W. (1 Ryd^{-1} = 0.484 as).

Table 1. Dependence of the spin-relaxation time on disorder in Cu. Also shown is the resistivity, ρ, diffusion coefficient, D and spin diffusion length l_{sf}.

W (eV)	ρ ($\mu\Omega$cm)	D 10^{-3}m^{2}s^{-1}	τ_{sf} (ps)	l_{sf} (nm)
0.0	0	∞	∞	∞
0.5	3.2	6.50	25.0	404
1.0	12.8	1.60	6.0	99
3.0	115	0.18	2.4	21

Figure 2 shows the time-evolution of the spin-polarisation integrated over the entire system as a function of time for disorder levels ranging from 0 to 3 eV. In the absence of disorder there is no spin-relaxation and this is in agreement with the Elliot-Yafet theory. At finite disorder the spin-polarised density decays in time. Interestingly there are fluctuations in the decay which become larger at increased levels of disorder. The probable cause for this effect is local variations in the spin-polarised density. The spin-relaxation times are extracted by fitting the tail of the decay to an exponential form. Table 1 summarises the fitted spin-relaxation times as a function of disorder together with appropriate resistivities and estimated spin-diffusion lengths.

The calculated spin-relaxation time at the realistic level of disorder, 0.5 eV, is 25 ps. The spin-diffusion length can be estimated by calculating the diffusion coefficient using the Einstein relation. The density of states at the Fermi energy in the TB copper model, $g(E_\mathrm{F}) = 1.87 \times 10^{47}$ J^{-1}m^{-3}, together with the resistivity define a spin-averaged diffusion coefficient, $D = 0.0065$ m^{2}s^{-1}.

The spin-diffusion length, l_{sf}, can be estimated using,

$$l_{\mathrm{sf}} = (D\tau_{\mathrm{sf}})^{\frac{1}{2}}, \tag{12}$$

which is the r.m.s. distance traveled before a spin-flip. Importantly there is a dual effect of disorder on spin-diffusion lengths. Increased disorder decreases the diffusion coefficient by increasing the spin-independent scattering of conduction electrons. It also decreases the spin-relaxation time in accordance with the Elliott-Yafet theory. For copper the spin-diffusion length is estimated to be 404 nm. This figure is in very good agreement with experimental evidence; transport measurements have determined the spin-diffusion length in Cu to vary between 350 nm and 1 μm between 4.2 K and room temperature [13].

4.2 Spin relaxation in nanocrystallite Cu

Spintronic devices often include components which are nanoscale in at least one dimension and in some cases all dimensions. It is important to understand the effect this can have on spin-relaxation and to that end we consider the same Cu system as discussed above but with box boundary conditions and with no Anderson disorder. In this case approximately 7% of the atoms in the system are surface atoms. Following the same procedure as previously detailed the spin-relaxation is simulated and Figure 3 shows the time-evolution of the spin-polarised density. In this case there is a significant effect corresponding to a spin-relaxation time of 0.47 ps. Notably the fluctuations observed in the case of Anderson disorder induced spin-relaxation are much reduced giving further support to idea that fluctuations are caused by local variations in spin-density. Spin-relaxation in this system occurs because of the translational symmetry breaking of the surface and for 7% surface atoms corresponds to a spin diffusion length that is much reduced compared the bulk, 55 nm compared to 404nm for bulk Cu with realistic resistivity.

4.3 Spin injection simulation

As an indication of how spin-relaxation effects may be incorporated into the EOM transport simulation a simple system is presented. A small crystal of copper is considered with periodic boundary conditions in the transverse x and y directions and current flow is along the z-direction (which is the (001) direction in the crystal). The system contains a total of 1960 atoms, with each transverse plane containing 98 atoms and with 20 planes in the current direction (corresponding to about 34 Å). A spin-polarised current is injected into system by using spin-dependent source magnitudes on the left boundary. The spin-orbit constants for this system are taken to be quite large ($\xi_p = 5$ eV and $\xi_d = 1$ eV) to cause significant spin-relaxation over the quite small length considered. Different levels of Anderson disorder are simulated corresponding to different values of W/V. Figure 4 shows

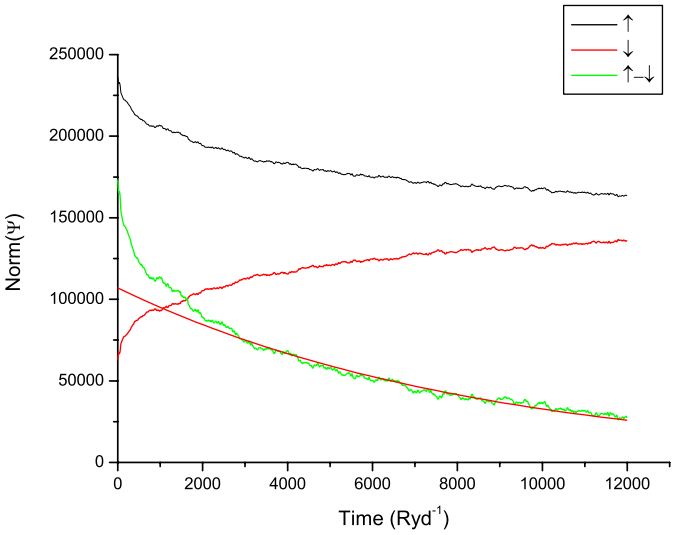

Fig. 3. Spin-relaxation in a finite nanocrystallite of Cu with 7% surface atoms.

the norm of the wavefunction for each spin channel averaged over the transverse planes in steady state.

At zero disorder (ballistic transport) there is a difference in the spin density which remains on the average constant throughout the system. As the disorder is increased two effects are apparent. The slope of the curves increases representing the increased resistance, and the two curves approach one another due to spin-relaxation. At the highest level of disorder the spin-diffusion length is so small that the spin-polarisation of the injected current disappears almost immediately. This very simple demonstration shows how the effects of spin-relaxation can be incorporated into transport calculations and is an important area for future work.

5 Conclusions

Quantum simulations of electronic transport and spin-relaxation in the presence of the spin-orbit interaction have been presented. The calculation of spin-relaxation times is very important from the point of view of spintronic device applications. It provides independent evidence separate from optical and transport measurements and could potentially suggest new materials which may be useful for maintaining spin coherence within devices. The simulated spin-relaxation in Cu is in reasonable agreement with experiments indicating that the approach based upon a TB parameterisation is justified. The simulation of spin-relaxation in a finite crystal has revealed a very significant effect due to the surface, and this is an issue to be considered for future nano-spintronic devices. The incorporation of the spin-orbit interaction and the effects of spin-relaxation into a quantum EOM method for electronic transport has many advantages. The ability to include dynamic effects is vital for simulations of spin-current driven magnetisation reversal for instance.

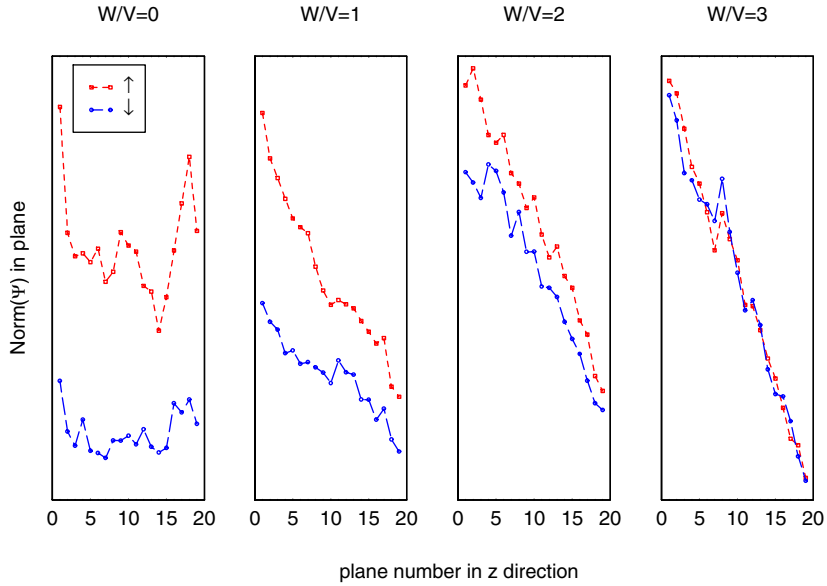

Fig. 4. Injection of a spin-polarised current into Cu with strong spin-orbit coupling($\xi_p = 5$ eV and $\xi_d = 1$ eV). As disorder in increased (from left to right) the spin-diffusion length is reduced.

An electronic structure based calculation such as the one presented here has the advantage that ferromagnetic materials may be studied without additional complexity, whereas transport measurements of spin-relaxation in ferromagnetic materials are more problematic. One can expect more complex and subtle behaviour in materials such as cobalt for example. The presence of the *d*-band just below the Fermi energy may cause sensitive dependence on disorder. As disorder is increased it may bring *d*-levels in the majority band closer to the Fermi energy. This could allow *d*-levels in the minority band to couple more strongly to the majority band through the spin-orbit interaction, and this could have a dramatic effect on spin-relaxation.

References

1. E.Y. Tsymbal, D.G. Pettifor, *Solid State Physics* (Academic Press, San Diego, 2001), Vol. 56, pp. 113–237
2. S.S.P. Parkin et al., J. Appl. Phys. **85**, 5828 (1999)
3. J.F. Gregg, I. Petej, E. Jouguelet, C. Dennis, J. Phys. D: Appl. Phys. **35**, R121 (2002)
4. F.J. Albert et al., Phys. Rev. Lett. **89**, 226802 (2002)
5. J. Fabian, S.D. Sarma, J. Vac. Sci. Technol. **17**, 1708 (1999)
6. K.P. McKenna, L.A. Michez, G.J. Morgan, B.J. Hickey, Phys. Rev. B **72**, 054418 (2005)
7. L.I. Schiff, *Quantum Mechanics* (McGraw-Hill, 1968)
8. R.J. Elliott, Phys. Rev. **96**, 266 (1954)
9. Y. Yafet, Solid State Physics **14**, 1 (1963)
10. J. Fabian, S.D. Sarma, Phys. Rev. Lett. **81**, 5624 (1998)
11. F. Beuneu, P. Monod, Phys. Rev. B **13**, 3424 (1976)
12. A.Y. Elezzabi, M.R. Freeman, M. Johnson, Phys. Rev. Lett. **77**, 3220 (1996)
13. F.J. Jedema, A.T. Filip, B.J. van Wees, Nature **410**, 345 (2001)
14. T. Valet, A. Fert, Phys. Rev. B **48**, 7099 (1993)
15. D.A. Papaconstantopolous, *Handbook of the bandstructure of elemental solids* (Plenum Press, 1986)
16. P. Butcher, J. Phys. C **5**, 3164 (1972)
17. F. Herman, S. Skillman, *Atomic structure calculations* (Prentice-Hall, 1963)
18. J. Friedel, J. Phys. Chem. Solids **25**, 781 (1964)
19. B. Kramer, A. MacKinnon, D. Weaire, Phys. Rev. B **23**, 6357 (1981)
20. B.J. Hickey, J.N. Burr, G.J. Morgan, Phil. Mag. Lett. **61**, 161 (1990)
21. P.W. Anderson, Phys. Rev. **109**, 1492 (1958)
22. E.Y. Tsymbal, D.G. Pettifor, Phys. Rev. B **54**, 15314 (1996)